

ARTICLE



A new photodynamic therapy photosensitizer (p1) promotes apoptosis of keloid fibroblasts by targeting caspase-8

Ming-Zi Zhang^{a*}, Xin-Hang Dong^{b*}, Wen-Chao Zhang^a, De-Li Pan^c, Li Ding^d, Hao-Ran Li^b, Peng-Xiang Zhao^e, Meng-Yu Liu^e, Lou-Bin Si^a, Xiao-Jun Wang^a , Xiao Long^a and Yi-Fang Liu^f

^aDepartment of Plastic Surgery, Peking Union Medical College Hospital, Beijing, China; ^bPlastic Surgery Hospital, Chinese Academy of Medical Sciences and Peking Union Medical College, Beijing, China; ^cDepartment of Radiology, Traditional Chinese Medicine Hospital of Huangdao district of Qingdao, Shandong, China; ^dDepartment of Planned Immunity, Changjianglu Community Health Center of the West Coast New Area, Qingdao, China; ^eCollege of Life Science and Bioengineering, Beijing University of Technology, Beijing, China; ^fInternational Education College, Beijing Vocational College of Agriculture, Beijing, China

ABSTRACT

Photodynamic therapy (PDT) is a new therapy for treating cancer with less toxicity, high selectivity, good cooperativity, and repetitive usability. However, keloid treatment by PDT is mainly focused on clinical appearance, and few studies have been conducted on the mechanisms of PDT. In this study, key factors of the classical mitochondrial apoptosis signaling pathway were measured to assess the effect of a new PDT photosensitizer (p1). A specific inhibitor of caspase-8 (Z-IETD-FMK) was also used to verify the possible mechanisms. Twelve samples were obtained from 12 patients (six with keloids and six without) selected randomly from the Department of Plastic Surgery at Peking Union Medical College Hospital from January to December 2020. After cell culture, fibroblasts were divided into 13 groups. The morphology of fibroblasts in each group was observed by microscopy. Cell activity was measured by cell counting kit-8, and cell apoptotic morphology was observed by TUNEL staining. The reactive oxygen species (ROS) relative value was measured by a ROS test kit. The expression levels of key mitochondrial factors (caspase-3, caspase-8, cytochrome-c, Bax, and Bcl-2) were assessed by western blot, and mRNA expression of caspase-3 and caspase-8 was measured by RT-qPCR. We showed that p1 had a satisfactory proapoptotic effect on keloid fibroblasts by increasing the expression of ROS, caspase-3, caspase-8, and cytochrome-c, and decreasing the Bcl-2/Bax ratio; however, this effect was partially inhibited by Z-IETD-FMK, indicating that caspase-8 may be one of the p1's targets to achieve the proapoptotic effect.

ARTICLE HISTORY

Received 28 February 2022
Accepted 19 April 2022

KEYWORDS

Keloid; photodynamic therapy; photosensitizer; apoptosis; mechanisms

Introduction

Keloid, which is considered a benign tumor, brings unbearable itch and pain, which seriously affects patients' quality of life. The most common clinical treatment for keloid is operation combined with other adjuvant therapy, such as radiation therapy or injection therapy, which is accompanied by many complications [1]. Therefore, it is necessary to find a new therapeutic approach with certain effectiveness and fewer complications.

Photodynamic therapy (PDT) is used for treating superficial cancer since 1993; it shows satisfactory characteristics, such as less toxicity, high selectivity, good cooperativity, and repetitive usability [2,3]. In 2011, Nie et al. discussed the potential application of PDT for keloid and suggested its mechanisms of action [4]. Since then, PDT has been considered a new therapy for treating keloid. However, previous studies have mainly focused on the clinical effect of PDT for keloids, and few studies have investigated molecular biological mechanisms at the cellular level. Therefore, we conducted the current study, where we chose a new type of photosensitizer (p1) and investigated its effects and possible mechanisms toward keloid fibroblasts by measuring the expression levels of key factors in the classical mitochondrial

apoptosis signaling pathway (caspase-3, caspase-8, cytochrome-c, Bax, and Bcl-2).

Materials and methods

Patient grouping, sample management, and cell culture

The Bioethical Committee of Peking Union Medical College Hospital reviewed and approved the study protocol. All patients signed informed consent. Twelve patients (six with keloid and six without keloid; three women and three men in each of the patient groups) were randomly selected at the Department of Plastic Surgery, Peking Union Medical College Hospital, from January to December 2020. The patients' age ranged from 20 to 55 years (patients with keloid: 35.68 ± 8.12 years; patients without keloid: 36.12 ± 7.57 years). All samples were located in the chest area. Each keloid had been caused by trauma and was diagnosed by pathological examination. None of the patients had any systemic diseases or were receiving any drugs that might have affected the results. No significant differences in basic characteristics were found between the patient groups.

CONTACT Lou-Bin Si  siloubin@vip.126.com  pumchwxj@163.com

*co-first authors.

In this study, cell culture was performed after obtaining a central part of keloid tissue and normal skin tissue. Excessive fat tissue, hair, and blood were removed, and the specimens were washed in phosphate-buffered saline (PBS). Keloid tissue specimens were cut into blocks of 0.2–0.3 cm³ and were laid onto 75-cm² culture flasks with 5–7 ml of Dulbecco's minimal essential medium (Gibco, Big Cabin, OK, USA) with 10% fetal bovine serum (Gibco), penicillin (100 U/mL), and streptomycin (100 µg/mL). The flasks were incubated at 37°C in an atmosphere of 5% carbon dioxide [5]. Normal skin fibroblast cell culture procedures were conducted in accordance with Vangipuram's study [6].

In this study, the concentration of the new PDT photosensitizer (p1) was 1.686 µM. The light condition included treatment with a 532 nm semiconductor laser (20 mW/cm² for 10 min). The concentration of Z-IETD-FMK was 50 µM. Thirteen different cell groups were involved: (1) N + p1: normal skin fibroblasts with p1; (2) N + light: normal skin fibroblasts under the light condition; (3) N + p1 + light: normal skin fibroblasts with p1 under the light condition; (4) N-con: normal skin fibroblasts; (5) K + p1: keloid fibroblasts with p1; (6) K + light: keloid fibroblasts under the light condition; (7) K + p1 + light: keloid fibroblasts with p1 under the light condition; (8) K-con: keloid fibroblasts; (9) K + Z-IETD-FMK: keloid fibroblasts with Z-IETD-FMK; (10) K + DMSO: keloid fibroblasts with solvent of Z-IETD-FMK (DMSO); (11) K + Z-IETD-FMK + p1 + light: keloid fibroblasts with Z-IETD-FMK and p1 under the light condition; (12) K + Z-IETD-FMK + p1: keloid fibroblasts with Z-IETD-FMK and p1; (13) K + Z-IETD-FMK + light: keloid fibroblasts with Z-IETD-FMK under the light condition. Fibroblasts of passage 3 were used for analysis. All evaluations were conducted 72 h after the intervention.

Microscope and TdT-mediated dUTP-X nick end labeling (TUNEL) staining observation

At 72 h after the intervention, cell morphology was observed by a microscope (100×). TUNEL staining was used to observe programmed cell death through a TUNEL detection kit (Appligen, Beijing, China). Fibroblasts were seeded at 2000 cells/well in 96-well plates for 72 h after the intervention. The staining procedures were based on kit instructions.

Cell activity evaluation

CCK-8 assay (Dojindo, Kumamoto, Japan) was used for cell activity evaluation at 2 h, 4 h, 8 h, 12 h, 24 h, 48 h, and 72 h after the intervention. Fibroblasts were seeded at 5000 cells/well in 96-well plates. The procedures were based on the kit's instructions, and the data were measured at 450 nm by a microplate reader. The trend of cell activity was recorded.

Reactive oxygen species (ROS) assessment

The relative value of ROS was assessed by a ROS detection kit (Beyotime, Shanghai, China) at 72 h after the intervention. The data were measured at 488 nm by a microplate reader. The relative value of ROS was calculated as ROS absorbance divided by protein quantity, in accordance with the kit instructions.

Real-time quantitative PCR (RT-qPCR) detection

The mRNA expression levels of caspase-3 and caspase-8 were also detected by the RT-qPCR technique. Total RNA Extraction Kit (Genesee, Guangzhou, China) and cDNA Synthesis Kit (New

Table 1. The sequences of the primers used for RT-qPCR.

Target gene	Forward	Reverse
Caspase-3	5'-TTGAGCCTGAGCAGAGACAT-3'	5'-CAGCATCATCCACACATACCA-3'
Caspase-8	5'-AACAGATGCCTCAGCCTACTT-3'	5'-GGCGACAGAGCGGATTCT-3'
GAPDH	5'-GGACTCATGACCACAGTCCA-3'	5'-TCAGCTCAGGGATGACCTTG-3'

England Biolabs, MA, USA) were used for the detection of mRNA expression. PCR was performed by using a Real-Time qPCR system (Agilent, Santa Clara, CA, USA). The sequences of the specific sets of primers for caspase-3, caspase-8, and GAPDH are shown in Table 1.

Western blot assessment

The protein extraction and western blot protocols were performed in accordance with our previous study [7]. Cell Total Protein Extraction Kit (Bio-Rad Laboratories, CA, USA) was used in this study. The protein membranes were incubated with anti-caspase-3 (1:500, Abcam, Cambridge, United Kingdom), anti-caspase-8 (1:200, Abcam), anti-Bax (1:200, Abcam), anti-Bcl-2 (1:200, Abcam), and anti-cytochrome-c (1:200, Abcam) at 4°C for 12–16 h. A secondary antibody (Li-cor, Lincoln, NB) at 1:10000 was used afterward. Protein density detection was measured by a double-color infrared laser imaging system (Odyssey, Li-cor).

Statistical analysis

Data in this study were presented as mean ± standard deviation (mean ± SD). The statistical analysis was conducted in SPSS Statistics 24.0 software (SPSS, Inc., Chicago, IL) through one-way analysis of variance (ANOVA) followed by the LSD *t*-test, and *p* < 0.05 was considered significant.

Results

Cell morphological observation

The cell morphological appearance at 72 h after the intervention was observed on a microscope. The cells of the K + p1 + light group showed typical signs of apoptosis, such as cell shrinkage, chromatin pyknosis, and karyorrhexis. In TUNEL staining images, more TUNEL-positive cells (red staining) were observed in the K + p1 + light group. In addition, cells in the N + p1 + light group showed more TUNEL-positive cells; however, their morphological appearance was not typical for apoptosis. In the K + Z-IETD-FMK + p1 + light group, the cell morphological appearance was not typical for apoptosis; however, TUNEL-positive cells were less frequent than in the K + p1 + light group and more frequent than in the other groups (Figure 1).

The trend of cell activity changes in different groups

The trend of cell activity changes in different groups is shown in Figure 2, displaying that the cell activity increased with time in all of the groups. At 48 h after the intervention, the cell activity of the K + p1 + light group differed significantly from those of the other K groups (*p* < 0.01). The difference became more obvious at 72 h after the intervention (*p* < 0.001). Compared with the K + p1 + light group, cell activity in the K + Z-IETD-FMK + p1 + light group was much higher (*p* < 0.001), yet it was obviously lower compared with the K-con group (*p* < 0.001). Compared with the K groups, the cell activity of the N groups was much lower (*p* < 0.001), while no significant differences were found among the N groups.

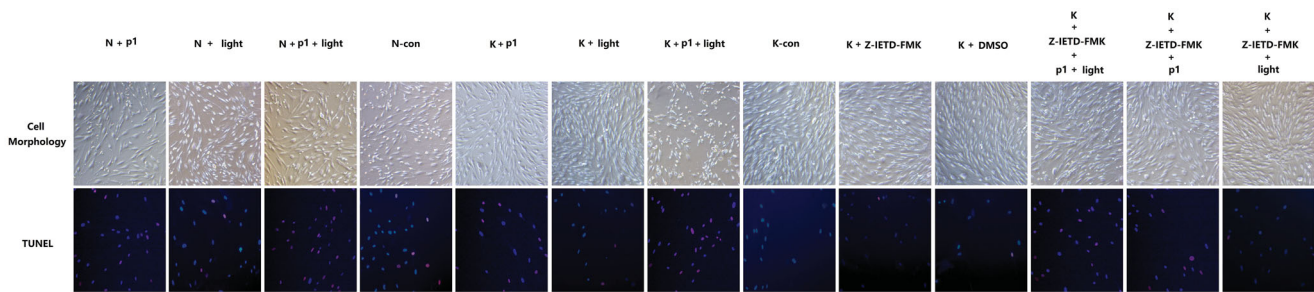


Figure 1. Fibroblasts' morphology and TUNEL staining images (100 \times) at 72h after intervention. Fibroblasts in the K + p1 + light group showed typical signs of cell apoptosis (cell shrinkage, chromatin pyknosis, and karyorrhexis) and a higher proportion of TUNEL-positive cells. Red staining indicates the TUNEL-positive cells.

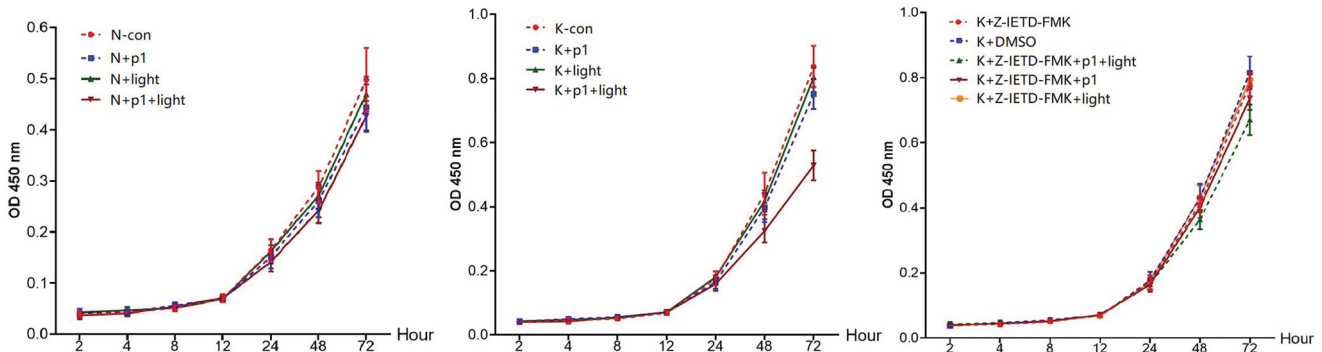


Figure 2. The trend of cell activity in different groups. Compared with the K-con group (48 h: 0.4408 ± 0.0656 ; 72 h: 0.8372 ± 0.0647), keloid fibroblasts' activity in the K + p1 + light group (48 h: 0.3246 ± 0.0362 , $p < 0.01$; 72 h: 0.5290 ± 0.0463 , $p < 0.001$) was remarkably lower at 48 h after the intervention. Values are shown as means \pm SD; ($n = 6$ in each group).

ROS production evaluation

Figure 3 shows the production of ROS among different groups. Compared with the K-con group, ROS production was remarkably higher ($p < 0.001$) in the K + p1 + light group and the K + Z-IETD-FMK + p1 + light group. However, compared with the K + p1 + light group, ROS production in the K + Z-IETD-FMK + p1 + light group was significantly lower ($p < 0.001$). In addition, ROS production in p1 groups was higher ($p < 0.01$) than that in non-p1 groups. No significant differences were found among the non-p1 groups. Similar ROS production was found between the K-con group and the K + DMSO group.

mRNA expression of caspase-3 and caspase-8

Figure 4 shows the mRNA expression levels in each of the groups. Among the K groups, the expression of caspase-8 mRNA was significantly higher ($p < 0.001$) in the K + p1 + light group compared with other K groups. Among the K groups (except for the K + Z-IETD-FMK + p1 + light group), the expression level of caspase-3 mRNA was much higher ($p < 0.001$) in the K + p1 + light group. Compared with the K + p1 + light group, mRNA expression of caspase-8 was significantly lower ($p < 0.001$) in the K + Z-IETD-FMK + p1 + light group, and did not differ significantly from that in the K-con group. In addition, mRNA expression of both caspase-3 and caspase-8 was higher ($p < 0.001$) in the N + p1 + light group compared with other groups.

Protein expression of key factors of apoptosis pathway

Figure 5 shows protein expression levels of caspase-3, caspase-8, cytochrome-c, Bcl-2, and Bax in the mitochondrial apoptosis signaling pathway. Among all of the K groups, higher caspase-3, caspase-8, cytochrome-c, and Bax expression levels, a lower Bcl-2

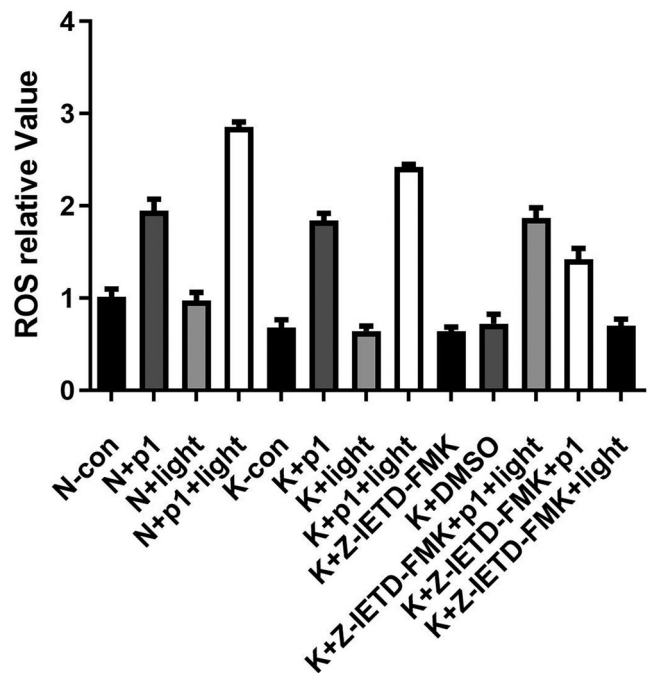


Figure 3. ROS production in different groups. Compared with the K-con group (0.6797 ± 0.0854), increased ROS production was shown in the K + p1 + light group (2.4210 ± 0.0288 , $p < 0.001$) and K + Z-IETD-FMK + p1 + light group (1.8673 ± 0.1105 , $p < 0.001$). No significant differences were found among the non-p1 groups. Values are shown as means \pm SD; ($n = 6$ in each group).

expression level, and a reduced Bcl-2/Bax ratio were found in the K + p1 + light group ($p < 0.001$). As for the K + Z-IETD-FMK + p1 + light group, the expression levels of caspase-3, caspase-8, cytochrome-c, Bcl2, and Bax, and the Bcl-2/Bax ratio were

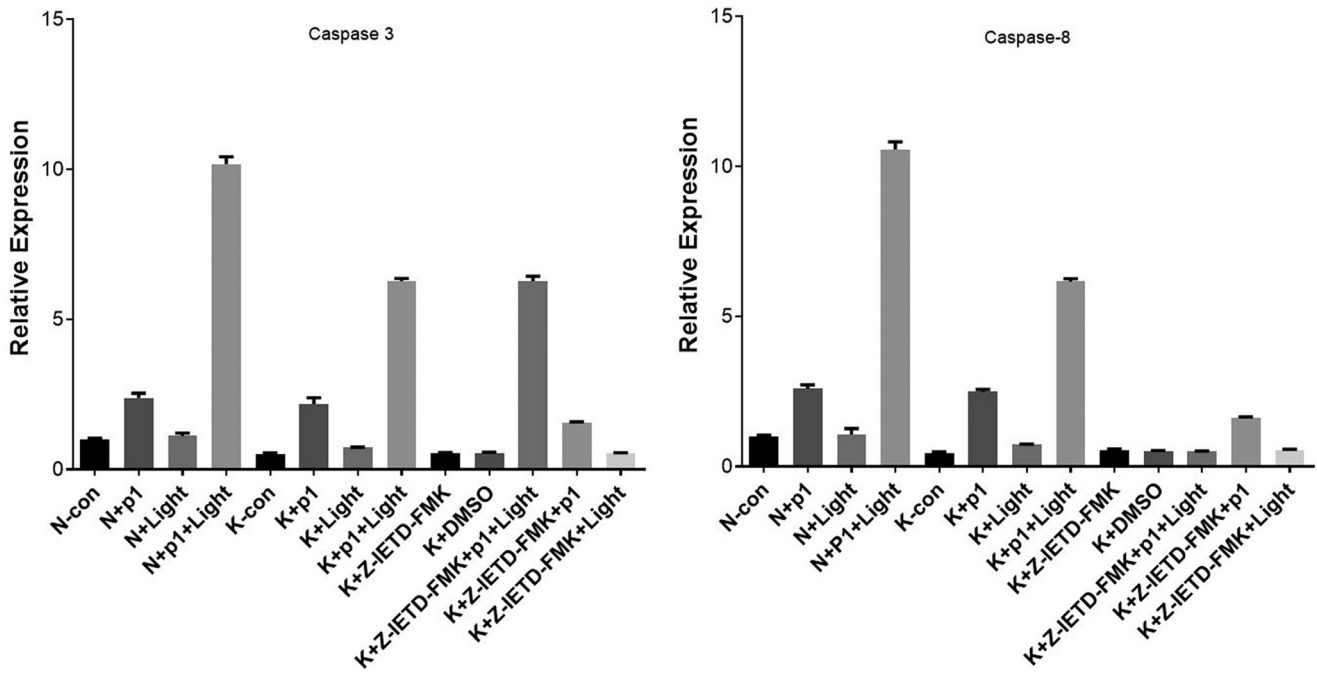


Figure 4. The mRNA relative expression levels of caspase-3 and caspase-8 in all of the groups. Compared with the K-con group, mRNA expression of caspase-3 (6.2771 ± 0.0870 , $p < 0.001$) and caspase-8 (6.1621 ± 0.0886 , $p < 0.001$) was significantly higher in the K + p1 + light group. Compared with the K + p1 + light group, Z-IETD-FMK significantly decreased the caspase-8 mRNA expression in the K + Z-IETD-FMK + p1 + light group (0.5049 ± 0.0193 , $p < 0.001$). Values are shown as means \pm SD; ($n = 6$ in each group).

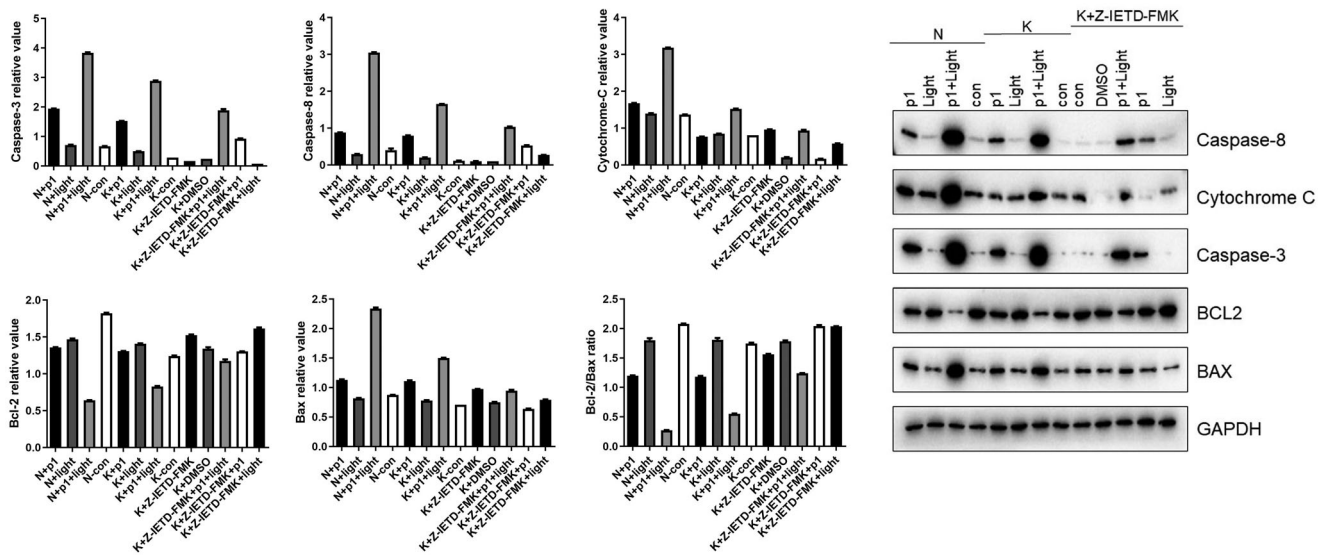


Figure 5. Protein expression of key factors in all of the groups. The key factors of the mitochondrial apoptosis pathway involve caspase-3, caspase-8, cytochrome-c, Bcl-2, and Bax. Among all of the keloid groups, the highest expression of caspase-3 (2.8802 ± 0.0198), caspase-8 (1.6504 ± 0.0053), cytochrome-c (1.5179 ± 0.0101), and Bax (1.5016 ± 0.0046), and the lowest Bcl-2 (0.8276 ± 0.0071) expression and Bcl-2/Bax ratio (0.5511 ± 0.0055) were found in the K + p1 + light group ($p < 0.001$). Compared with the K + p1 + light group, Z-IETD-FMK significantly decreased the expression of caspase-8 (1.0313 ± 0.0119 , $p < 0.01$) in the K + Z-IETD-FMK + p1 + light group. Values are shown as means \pm SD; ($n = 6$ in each group).

located in the middle between the K-con group ($p < 0.001$) and the K + p1 + light group ($p < 0.01$). Among all of the groups, the highest expression levels of caspase-3, caspase-8, cytochrome-c, and Bax, and the lowest expression of Bcl-2 and Bcl-2/Bax ratio were found in the N + p1 + light group.

Discussion

Although keloid is considered a benign tumor, its growth characteristics may bring obvious clinical symptoms that seriously affect

patients' quality of life [8,9]. So far, the mainstream treatment is operation combined with adjunctive therapies. Many adjunctive therapies have been used, such as radiation therapy, injection therapy, pressure therapy, and others [10]. In our previous study, we have concluded that keloid may be in a state of imbalance between a high proliferation level and a relatively low apoptosis level, which causes continuous growth characteristics [7,11]. In this context, pro-apoptosis may be an efficient way of treating keloid.

PDT is a therapeutic method that applies a certain wavelength of light to stimulate the photosensitizer gathered at the tumor to

produce ROS and lead to cell death [12,13]. In former studies, researchers identified three main factors that may decide the effect of PDT: oxygen, photosensitizer, and light [14]. The mechanism of PDT has not been fully studied, but it is believed that PDT participates in many biological processes under light activation, including cell necrosis, apoptosis, and immunogenic cell death [15]. In addition, PDT has also been used in a clinical setting and has shown satisfying treatment effects, especially in actinic keratosis, Bowen disease, basal cell carcinoma, viral warts, liver malignancies, and colorectal cancer [16–18]. Nie treated keloids with five sessions of methyl aminolevulinate PDT over a period of five months, which was effective [19]. Ud-Din also applied PDT in keloid treatment and found that PDT with minimal side effects was able to reduce scar formation by decreasing blood flow, increasing pliability, and decreasing collagen and hemoglobin levels [20]. In 2020, Tosa reviewed the use of PDT in keloids and concluded that PDT may play a promising role in keloid treatment [21]. In recent years, clinical studies of PDT have been conducted, but the mechanisms are still not fully understood.

As mentioned above, the photosensitizer is one of the key points in PDT. In former studies, p1 showed an improved treatment effect with satisfying water solubility and convenient preparation [22,23]. In this study, we investigated the proapoptotic effect and possible mechanisms of new photosensitizer p1 toward keloid fibroblasts.

In microscopic observation, keloid fibroblasts showed a typical apoptosis appearance (cell shrinkage, chromatin pyknosis, and karyorrhexis) and more TUNEL-positive cells after p1 intervention under the light condition, indicating that p1 had a proapoptotic effect at the morphological level. As shown by the CCK-8 assay, the activity of keloid fibroblasts was significantly inhibited at 48 h and 72 h after the intervention, which is an aspect to evaluate the p1's action intensity. The new photosensitizer p1 accompanied by oxygen and light was able to efficiently convert oxygen into ROS and initiate the apoptosis pathway. The cells produced more ROS by p1 under the light condition, which is similar to former studies' results [24]. The mitochondrial apoptosis pathway is a classic apoptosis pathway; it involves key factors such as caspase-3, caspase-8, cytochrome-c, Bcl-2, and Bax. In addition, Bcl-2/Bax usually determines the direction of apoptosis [25–27]. In protein expression results, proapoptotic factors (caspase-3, caspase-8, cytochrome-c, Bax) were significantly increased and the Bcl-2/Bax ratio was decreased by p1 under the light condition. These results indicated that p1 under the light intervention was able to effectively promote cell apoptosis at the morphological level and molecular biological level. Cui et al. also indicated the proapoptotic effect of PDT based on the increased expression of caspase-3 [28]. At the mRNA level, p1 under the light condition also increased the mRNA expression levels of caspase-3 and caspase-8.

We further focused on caspase-8, the key factor in the mitochondrial apoptosis pathway, and used its specific inhibitor (Z-IETD-FMK) to test p1's action target. The results showed that Z-IETD-FMK was able to effectively inhibit the mRNA and protein expression of caspase-8. Comparing the results of the K+Z-IETD-FMK+p1+light group with the K-con group and the K+p1+light group, we concluded that fibroblast apoptosis was partially inhibited by Z-IETD-FMK, indicating that targeting caspase-8 may be one of the mechanisms of p1 in promoting keloid fibroblasts' apoptosis. We then established normal skin fibroblasts as control groups. Interestingly, the results showed that p1 under the light condition also showed a proapoptotic effect on normal skin fibroblasts at the molecular biological level but not at the morphological level. According to our former study [11], keloid

tissue has a much higher cell proliferation level than normal skin tissue. Considering our CCK-8 results, normal skin fibroblasts may be in a low activity state. In addition, Li et al. concluded that the high speed of intracellular transport dynamics is critical for promoting apoptosis [29]. Hence, normal skin fibroblasts may be in a low activity state due to inefficient intracellular transport, which firstly showed accumulation of protein and mRNA, while maintaining early apoptotic cell morphology. However, further research should be conducted to test this theory. In addition, all groups with p1 intervention without light showed a tendency to promote apoptosis (even if the degree was quite low). It is impossible to establish a fully dark environment during the experiment, so even poor light conditions may motivate p1 and induce weak proapoptotic effects.

Based on the results above, we can conclude that the new photosensitizer p1 is efficient in promoting keloid fibroblasts' apoptosis, and that caspase-8 may be one of its targets. Thus, p1 may be a promising drug for future keloid treatment. However, this study focused on its effect and mechanisms at the cellular level, and animal models should be used to verify its effects.

Disclosure statement

No potential conflict of interest was reported by the author(s).

Funding

This work has been supported by the National Natural Science Foundation of China [81801926 and 82102326].

ORCID

Xiao-Jun Wang  <http://orcid.org/0000-0002-1820-9086>

References

- [1] Cheraghi N, Cognetta A Jr, Goldberg D. Radiation therapy for the adjunctive treatment of surgically excised keloids: a review. *J Clin Aesthet Dermatol*. 2017;10(8):12–15.
- [2] Dolmans DEJGJ, Fukumura D, Jain RK. Photodynamic therapy for cancer. *Nat Rev Cancer*. 2003;3(5):380–387.
- [3] Dougherty TJ, Henderson BW, Gomer CJ, et al. Photodynamic therapy. *J Natl Cancer Inst*. 1998;90(12):889–905.
- [4] Nie Z. Is photodynamic therapy a solution for keloid? *G Ital Dermatol Venereol*. 2011;146(6):463–472.
- [5] Zhang MZ, Liu YF, Ding N, et al. 2-Methoxyestradiol improves the apoptosis level in keloid fibroblasts through caspase-dependent mechanisms *in vitro*. *Am J Transl Res*. 2018;10(12):4017–4029.
- [6] Vangipuram M, Ting D, Kim S, et al. Skin punch biopsy explant culture for derivation of primary human fibroblasts. *J Vis Exp*. 2013;7(77):e3779–e3781.
- [7] Zhang MZ, Dong XH, Guan EL, et al. A comparison of apoptosis levels in keloid tissue, physiological scars and normal skin. *Am J Transl Res*. 2017;9(12):5548–5557.
- [8] Kassi K, Kouame K, Kouassi A, et al. Quality of life in Black African patients with keloid scars. *Dermatol Reports*. 2020;12(2):8312–8315.
- [9] Lee HJ, Jang YJ. Recent understandings of biology, prophylaxis and treatment strategies for hypertrophic scars and keloids. *IJMS*. 2018;19(3):711–739.

- [10] Marneros AG, Krieg T. Keloids-clinical diagnosis, pathogenesis, and treatment options. *J Dtsch Dermatol Ges.* 2004; 2(11):905–913.
- [11] Zhang MZ, Dong XH, Zhang WC, et al. A comparison of proliferation levels in normal skin, physiological scar and keloid tissue. *J Plast Surg Hand Surg.* 2021;29:1–7.
- [12] Dobson J, de Queiroz GF, Golding JP. Photodynamic therapy and diagnosis: principles and comparative aspects. *Vet J.* 2018;233:8–18.
- [13] Donohoe C, Senge MO, Arnaut LG, et al. Cell death in photodynamic therapy: from oxidative stress to anti-tumor immunity. *Biochim Biophys Acta Rev Cancer.* 2019;1872(2): 188308.
- [14] Rkein AM, Ozog DM. Photodynamic therapy. *Dermatol Clin.* 2014;32(3):415–425.
- [15] Hou YJ, Yang XX, Liu RQ, et al. Pathological mechanism of photodynamic therapy and photothermal therapy based on nanoparticles. *Int J Nanomed.* 2020;15:6827–6838.
- [16] Liu D, Zhao S, Li J, et al. The application of physical pretreatment in photodynamic therapy for skin diseases. *Lasers Med Sci.* 2021;36(7):1369–1377.
- [17] Zou H, Wang F, Zhou JJ, et al. Application of photodynamic therapy for liver malignancies. *J Gastrointest Oncol.* 2020;11(2):431–442.
- [18] Yan J, Wang C, Jiang X, et al. Application of phototherapeutic-based nanoparticles in colorectal cancer. *Int J Biol Sci.* 2021;17(5):1361–1381.
- [19] Nie Z, Bayat A, Behzad F, et al. Positive response of a recurrent keloid scar to topical methyl aminolevulinate-photodynamic therapy. *Photodermatol Photoimmunol Photomed.* 2010;26(6):330–332.
- [20] Ud-Din S, Thomas G, Morris J, et al. Photodynamic therapy: an innovative approach to the treatment of keloid disease evaluated using subjective and objective non-invasive tools. *Arch Dermatol Res.* 2013;305(3):205–214.
- [21] Tosa M, Ogawa R. Photodynamic therapy for keloids and hypertrophic scars: a review. *Scars Burn Heal.* 2020;6:1–8.
- [22] Fang Y, Liu T, Zou Q, et al. Water-soluble benzylidene cyclopentanone based photosensitizers for *in vitro* and *in vivo* antimicrobial photodynamic therapy. *Sci Rep.* 2016; 6:28357.
- [23] Fang Y, Liu T, Zou Q, et al. Cationic benzylidene cyclopentanone photosensitizers for selective photodynamic inactivation of bacteria over mammalian cells. *RSC Adv.* 2015; 5(69):56067–56074.
- [24] Ming L, Cheng K, Cheng Y, et al. Enhancement of tumor lethality of ROS in photodynamic therapy. *Cancer Med.* 2021;10(1):257–268.
- [25] Estaquier J, Vallette F, Vayssiere JL, et al. The mitochondrial pathways of apoptosis. *Adv Exp Med Biol.* 2012;942: 157–183.
- [26] Jeong SY, Seol DW. The role of mitochondria in apoptosis. *BMB Rep.* 2008;41(1):11–22.
- [27] Li YN, Ning N, Song L, et al. Derivatives of deoxydoporphylotoxin induce apoptosis through bcl-2/bax proteins expression. *Anticancer Agents Med Chem.* 2021;21(5): 611–620.
- [28] Cui X, Zhu J, Wu X, et al. Hematoporphyrin monomethyl ether-mediated photodynamic therapy inhibits the growth of keloid graft by promoting fibroblast apoptosis and reducing vessel formation. *Photochem Photobiol Sci.* 2020; 19(1):114–125.
- [29] Li B, Dou SX, Yuan JW, et al. Intracellular transport is accelerated in early apoptotic cells. *Proc Natl Acad Sci USA.* 2018;115(48):12118–12123.